Received 16 January 2007
Revised 30 April 2007
Accepted 30 April 2007

# ISSUE 3: NUMERICAL HEAT TRANSFER IN PRACTICAL THERMAL SYSTEMS

# Numerical simulation of complex transport phenomena arising in practical thermal systems

Yogesh Jaluria
*Department of Mechanical and Aerospace Engineering, Rutgers, The State University of New Jersey, New Brunswick, New Jersey, USA*

## Abstract

**Purpose** – This paper seeks to discuss the numerical modeling of the transport processes that frequently arise in practical thermal systems and involve complexities such as property variations with temperature or with the shear rate in the flow, complicated regions, conjugate mechanisms, chemical reactions and combined mass transfer, and intricate boundary conditions.

**Design/methodology/approach** – The basic approaches that may be adopted in order to study such processes are discussed. Considerations for accurate numerical modeling are also discussed. The link between the process and the resulting product is critical in many systems such as those in manufacturing. The computational difficulties that result from the non-Newtonian behavior of the fluid or from the strong temperature dependence of viscosity are considered in detail. Similarly, complex geometry, free surface flow, moving boundaries, combined mechanisms, and simulation of appropriate boundary conditions are important in several processes and are discussed.

**Findings** – Some of the important techniques to treat the problems that arise in numerical simulation are presented. Common errors that lead to inaccurate or invalid results are outlined. A few practical processes are considered in greater detail to quantify and illustrate these approaches. Validation of the numerical model is a particularly important aspect and is discussed in terms of existing results, as well as development of experimental arrangements to provide inputs for satisfactory validation.

**Originality/value** – Practical thermal processes involve a wide variety of complexities. The paper presents some of the important ones and discusses approaches to deal with them. The paper will be of particular value to the numerical simulation of complicated thermal processes in order to design, control or optimize them to achieve desired thermal processing.

**Keywords** Simulation, Thermal testing, Numerical analysis

**Paper type** Research paper

## 1. Introduction

The numerical modeling of the complex transport phenomena that arise in various practical thermal systems and processes is discussed in this presentation. Complexities may be due to the material characteristics, such as those due to strong property variations with temperature or non-Newtonian behavior with the shear rate in the flow (Jaluria, 1996). Similarly, complicated computational domains and boundary conditions are of interest in many important processes (Paek, 1999). Additional mechanisms such as surface tension effects and chemical reactions are often important (Mahajan, 1996; Jaluria, 2001). In this paper, the governing equations, the relevant boundary conditions,

International Journal of Numerical Methods for Heat & Fluid Flow
Vol. 18 No. 3/4, 2008
pp. 288-307

0961-5539
DOI 10.1108/09615530810853592

and the basic approach to a numerical study of such processes are discussed. The importance of material characterization in an accurate mathematical and numerical modeling is brought out, along with the coupling between the process and the resulting properties. The various concerns and computational difficulties that arise due to the non-Newtonian behavior of the fluid, strong temperature dependence of viscosity, complex geometry, free surface flow, conjugate transport, and many other such effects, which are commonly encountered in practical processes, are considered. An object undergoing a given thermal transport process may be moving, with the velocity level changing significantly, as is the case for optical fiber drawing due to the large change in diameter (Paek, 1999; Jaluria, 1992). Some of the important methods to treat these problems and challenges are presented. Common errors that must be avoided are outlined. A few important practical processes, such as polymer extrusion, optical fiber drawing, enclosure fires, and cooling of electronic systems, are considered and characteristic numerical results presented and discussed. Special efforts made to accurately model the physical process are discussed. Validation of the numerical model is a very critical aspect and is discussed in detail, considering comparisons with existing analytical, numerical and experimental results (Roache, 1998). Development of experimental systems for providing the means for accurate validation of the model is also considered. The implications of an accurate and valid numerical simulation in improving existing practical thermal systems and in the design and optimization of future systems are discussed.

The various aspects mentioned above are extremely important in the analysis and simulation of a wide variety of engineering applications. However, these considerations have not received sufficient attention in the literature because of the computational complexities that arise. The governing equations are strongly coupled and large nonlinear effects arise that make analysis and numerical modeling very involved. It is important to develop strategies to mathematically and numerically model these processes and validate the models to ensure the accuracy. This paper considers several circumstances such as those that arise in the thermal processing of materials such as plastics, food, glass, composite materials and ceramics. In this case, the fluids involved are generally very viscous and the properties are very strongly dependent on the temperature. The computational domain is generally very complicated. Many transport mechanisms are quite involved and these are frequently coupled. The boundary conditions also tend to be very complicated and an accurate simulation of these is critical to the overall accuracy of the model. Similarly, in enclosure fires and cooling of electronic systems, the geometry is usually complicated, combined mechanisms arise and property variations are important.

Thus, this paper considers the numerical simulation of practical thermal processes and systems, focusing on the following major aspects that frequently arise:

- Large material property changes with temperature, shear rate, concentration and other parameters. This includes changes in the material characteristics and structure because of chemical reactions.
- Complicated geometry of the transport domain, including large changes in dimension.
- Boundaries such as free surfaces that not known initially and have to be determined as part of the solution.

- Intricate boundary conditions, including combined mechanisms operating at the boundaries, flow through openings and movement of surfaces.
- Validation of the mathematical/numerical model.

The basic approach to the treatment of these aspects is first outlined, indicating some of the common solution strategies and errors committed. This is followed by a presentation and discussion of characteristic results for a few important processes.

## 2. Analysis and numerical modeling

### *2.1 Governing equations*

The governing equations for most of the processes mentioned earlier are based on the usual conservation laws for mass, momentum and energy. A radiative source term arises for non-opaque materials like glass, since it emits and absorbs energy as function of the wavelength. Also, viscous dissipation effects are included for flow of highly viscous materials like polymers and glass due to the large viscosity of the material. The general equations may be written as:

$$\frac{\mathrm{D}\rho}{\mathrm{D}t} + \rho\nabla\cdot\bar{V} = 0 \tag{1}$$

$$\rho\frac{\mathrm{D}\bar{V}}{\mathrm{D}t} = \bar{F} + \nabla\cdot\tau \tag{2}$$

$$\rho C_p\frac{\mathrm{D}T}{\mathrm{D}t} = \nabla\cdot(k\nabla T)\dot{Q} + \beta T\frac{\mathrm{D}p}{\mathrm{D}t} + \mu\Phi \tag{3}$$

where $\rho$ is the density, $C_p$ is the specific heat at constant pressure, $k$ is the thermal conductivity, $\beta$ is the coefficient of volumetric expansion, $\dot{Q}$ is a thermal energy source per unit volume, $T$ is the temperature, $t$ is the time, $p$ is the pressure, and $\bar{F}$ is the body force per unit volume. Also, D/D$t$ is the substantial or particle derivative, given in terms of the local derivatives in the flow field as $\mathrm{D}/\mathrm{D}t = \partial/\partial t + \bar{V}\cdot\nabla$. The stress tensor $\tau$ in equation (2) can be written in terms of the velocity $\bar{V}$ if the fluid characteristics are known. For instance, if the dynamic viscosity $\mu$ is taken as constant for a Newtonian fluid, the relationship between the shear stresses and the shear rates, given by stokes, are employed to yield:

$$\rho\frac{\mathrm{D}\bar{V}}{\mathrm{D}t} = \bar{F} - \nabla_p + \mu\nabla^2\bar{V} + \frac{\mu}{3}\nabla(\nabla\cdot\bar{V}) \tag{4}$$

Here, the bulk viscosity $K = \lambda + (2/3)\mu$ is taken as zero. For an incompressible fluid, $\rho$ is constant. This gives $\nabla\cdot\bar{V} = 0$ from equation (1) and, thus, the last term in equation (4) drops out. Considering flow in a channel, if the flow is assumed to be developed in the down-channel, $z$, direction and lumping across the width is used, i.e. velocity varying only with distance $y$ from one wall of a channel to the other, the governing momentum equations become:

$$\frac{\partial p}{\partial x} = \frac{\partial\tau_{yx}}{\partial y}, \quad \frac{\partial p}{\partial y} = 0, \quad \frac{\partial p}{\partial z} = \frac{\partial_{yz}}{\partial y} \tag{5}$$

where the pressure terms balance the viscous forces.

The viscous dissipation term $\mu\Phi$ in equation (3) represents the irreversible part of the energy transfer due to the shear stress and is important in many practical processes. Viscous dissipation gives rise to a thermal source in the flow and is always positive. For a Cartesian coordinate system, $\Phi$ is given by the expression:

$$\Phi = 2\left[\left(\frac{\partial u}{\partial x}\right)^2 + \left(\frac{\partial v}{\partial y}\right)^2 + \left(\frac{\partial w}{\partial z}\right)^2\right] + \left(\frac{\partial v}{\partial x} + \frac{\partial u}{\partial y}\right)^2 + \left(\frac{\partial w}{\partial y} + \frac{\partial v}{\partial z}\right)^2 + \left(\frac{\partial u}{\partial z} + \frac{\partial w}{\partial x}\right)^2 - (\nabla \cdot \bar{V})^2 \quad (6)$$

Similarly, expressions for other coordinate systems may be obtained. This term becomes important for very viscous fluids or for flows at high speeds. The former circumstance is of particular interest in the processing of glass, plastics, food, and other polymeric materials. Similarly, energy input can be provided by chemical reactions, as is the case in combustion, chemical vapor deposition (Jensen *et al.*, 1991) and thermal processing of reactive polymers. The equations for the chemical species have to be solved, along with those for the flow and heat transfer, and a coupled heat and mass transfer problem usually arises. Then, an accurate simulation of the chemical kinetics is critical to a satisfactory and validated modeling of the process.

*2.2 Material properties*

Material properties are crucial to the accuracy of any numerical simulation. However, accurate property data are often not available and one has to resort to the information available. Frequently, these data are available at conditions, like the temperatures, that are different from those for the actual process, and thus severely limit the usefulness of the simulation. As an example, let us consider the manufacture of optical fibers. One of the most widely used methods for drawing optical fibers is based on heating a specially fabricated silica glass preform in a cylindrical furnace above its softening point $T_{\text{melt}}$ of around 1,900 K and pulling it into a fiber (Li, 1985). An axial draw tension is applied at the end of the preform so that the preform is drawn into a fiber through a neck-down region, as shown in Figure 1. The neck-down profile depends upon the drawing conditions, as well as on the physical properties of silica glass.

For glass, the material properties are strong functions of the temperature $T$. They also vary with composition and changes in the microstructure, the main effect being on the radiation properties and on the refractive index. The variation in the viscosity is the most critical one for the flow, since it varies quite dramatically with temperature. An equation based on the curve fit of available data for kinematic viscosity $v$ is written for silica, in S.I. units, as:

$$v = 4545.45 \exp\left[32\left(\frac{T_{\text{melt}}}{T} - 1\right)\right] \quad (7)$$

indicating the strong, exponential, variation of $v$ with temperature. Variations in all the other relevant properties of glass need to be considered as well, even though the variation with $T$ is not as strong as that of viscosity. The properties of the purge gas in the furnace may be considered to be constant since their variations are small over the temperature ranges encountered. Clearly, numerical models that can capture and

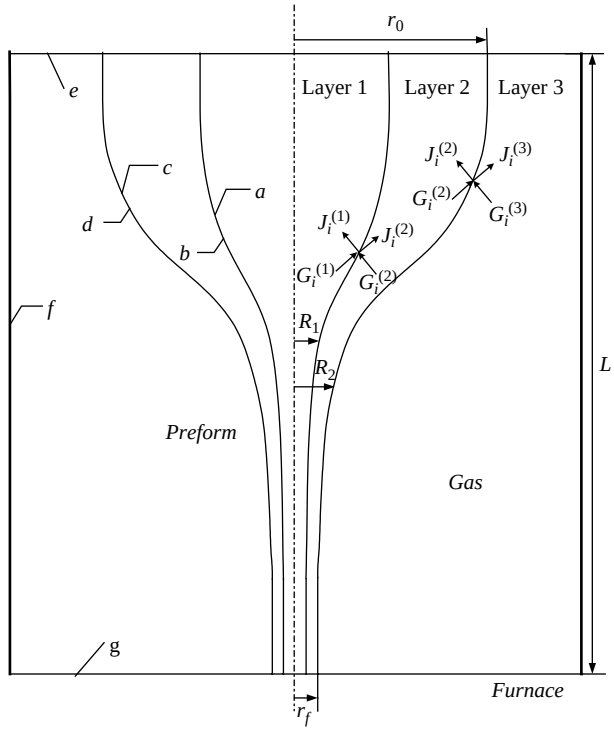


**Figure 1.**
Neck-down region for the drawing of a two-layer, core and cladding, optical fiber

represent such strong variations in the properties are necessary for an accurate simulation of this and other similar processes.

The radiative source term $\dot{Q}$ in equation (3) is non-zero for the glass preform/fiber because glass emits and absorbs energy. The variation of the absorption coefficient with wavelength $\lambda$ can often be approximated in terms of bands with constant absorption over each band. A two- or three-band absorption coefficient distribution can be effectively used, as shown in Figure 2. One of the methods that have been used successfully to model the radiative transport is the zone model (Yin and Jaluria, 1997). Other methods like the discrete ordinates method have also been used, though the major constraint has been the availability of accurate radiative property data.

Similarly, the transport processes in polymer processing or coating involve large material property changes. Since, the properties may vary with temperature and species concentration, the flow is coupled with the heat and mass transfer problem. However, most materials are also non-Newtonian and the viscosity varies with the shear rate and thus with the flow, making the problem even more complicated. The fluid viscosity is often taken as:

$$\mu = \mu_o \left(\frac{\dot{\gamma}}{\dot{\gamma}_o}\right)^{n-1} \exp\left(\frac{b}{T}\right) \tag{8}$$

where $\dot{\gamma}$ is the total strain rate, $b$ is the temperature coefficient of viscosity, subscript o indicates reference conditions and $n$ is the power-law index of the fluid. The extruded

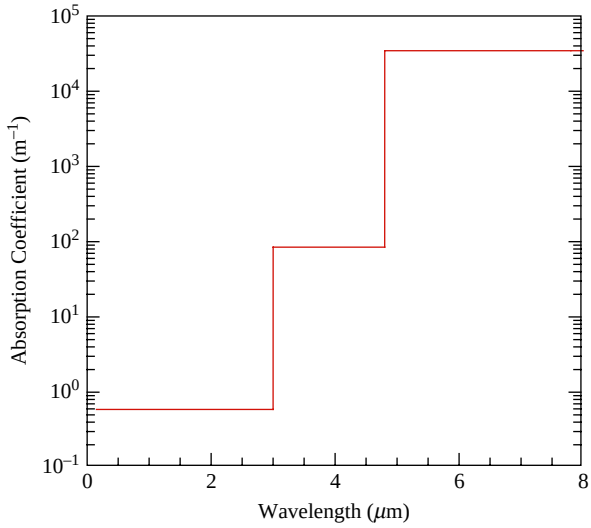


**Figure 2.**
Absorption coefficient of silica glass represented as a three-band model

material is thus treated as a generalized Newtonian-fluid (Tadmor and Gogos, 1979). For example, for a 2D flow, with velocity components $u$ and $w$ varying only with $y$:

$$\dot{\gamma} = \left[ \left(\frac{\partial u}{\partial y}\right)^2 + \left(\frac{\partial w}{\partial y}\right)^2 \right]^{1/2}, \text{with} \quad \tau_{yx} = \mu \frac{\partial u}{\partial y}, \quad \tau_{yz} = \mu \frac{\partial w}{\partial y} \tag{9}$$

For food materials, the rheological model becomes even more involved because of the dependence on the moisture concentration $C$. The changes in the chemical structure can also be included as a factor in these equations if experimental data are available. Other constitutive relations for viscosity can easily be employed instead, depending on the material.

*2.3 Complicated domains*

In many practical problems, the computational domain is very complicated. Various approaches, such as transformations and finite element methods, have been used for the numerical model. Optical fibers typically consist of a core and cladding, representing two silica glass compositions with a lower refractive index of the outer layer, as shown in Figure 1. The equations, as well as the boundary conditions, for both the glass and the purge gas regions may be transformed, by using Landau's transformation, to convert the computational domains to cylindrical ones, as shown in Figure 3 to simplify the discretization. Here, $R(z)$ is the radius of the perform/fiber as a function of the axial distance $z$. The transformation equations are also shown in the figure, with $r$ as the radial coordinate and z as the axial coordinate. Subscript F refers to the furnace, the superscripts to the different layers and $L$ to the furnace length.

Similarly, in single-screw extrusion of polymers, a rotating screw is located in a cylindrical barrel, with inflow of material at one end and a die for the outflow at the other. The geometry is very complicated and the rotation of the screw makes any simulation very involved. Frequently, the coordinate system is located on the rotating screw and curvature effects are neglected to give rise to steady flow in a channel with

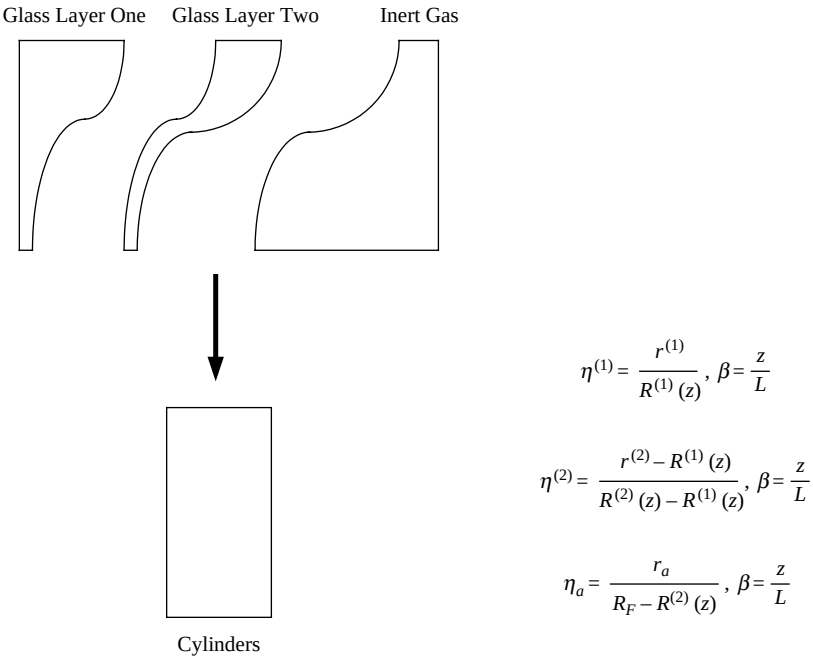


**Figure 3.**
Landau's transformation to convert the complicated axisymmetric regions in a fiber into cylindrical domains

the barrel moving at the pitch angle, as shown in Figure 4. The twin-screw extruder uses similar simplifications and involves channel flow and an intermeshing or mixing region. The governing equations are given in the references mentioned earlier for steady flow in screw channels completely filled with a rheological fluid.

*2.4 Boundary conditions*

In practical problems, the boundary conditions are frequently complicated and involve combined transport processes operating at the boundaries. It is extremely important to simulate the boundary conditions accurately since the entire simulation is strongly affected by the transport at the boundaries. For instance, the neck-down profile in optical fiber drawing is an unknown and must be obtained as a solution to the coupled transport equations in order to yield accurate results on the temperature and velocity profiles. In addition, the feasibility of the process is determined by the existence of a physically acceptable and stable neck-down profile (Roy Choudhury *et al.*, 1999). Owing to the complexity of determining the neck-down profile, several early investigators assumed the neck-down profile (Paek, 1999; Lee and Jaluria, 1996). Basically, the free-surface profile is the result of the various forces acting on the fiber. These include viscous, gravitational, surface tension and shear forces at the surface. Using force balance equations, along with the governing equations, the analysis must ensure that the radial and axial force balances are satisfied. The externally applied draw tension $F_T$ is obtained by considering an imaginary cut at an axial location z in the soft region of the neck-down and obtaining the force balance. Similarly, in the screw-extrusion of polymers, conjugate conditions due to conduction in the barrel and in the screw must be included at the channel boundaries (Lin and Jaluria, 1998).

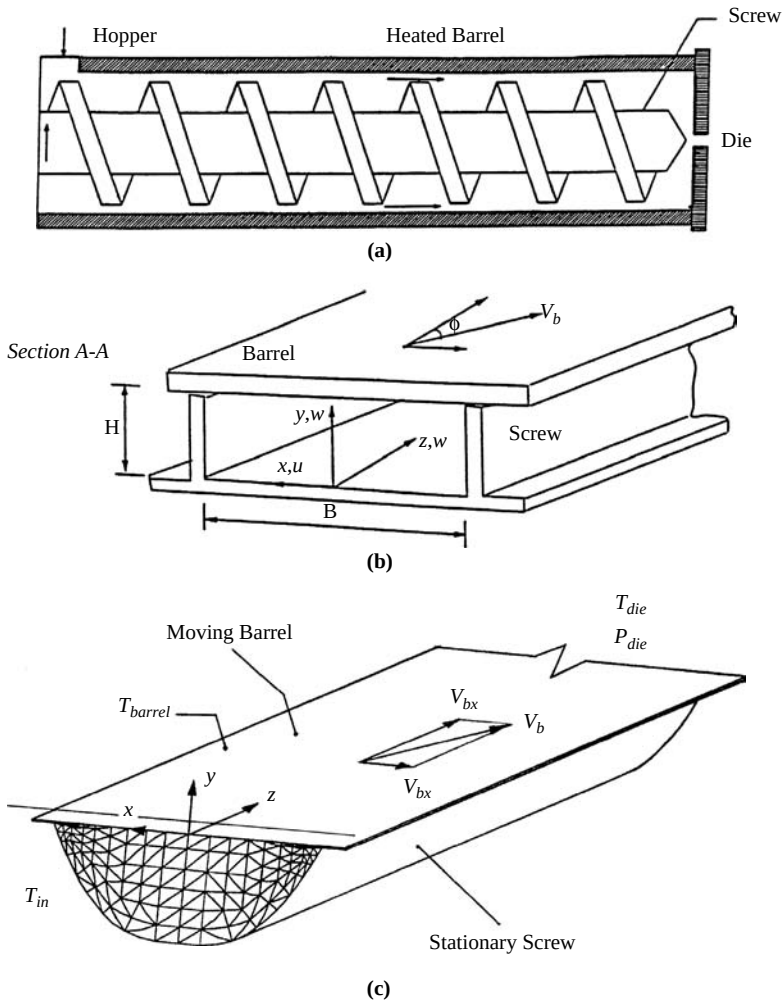


**Figure 4.**
Single-screw polymer extruder, shown as a channel flow obtained with the coordinate system fixed to the rotating screw and neglecting curvature effects

*2.5 Numerical solution*

Clearly, many of the processes mentioned here are complicated because of large property changes or because of chemical reactions and consequent changes in the material. In addition, the flow domain has a complicated geometry, made even more involved due to the movement of the boundary as is the case in polymer extrusion due to the rotation of the screws. The boundaries are complicated due to free surfaces, combined mechanisms, or unknown location and geometry. It is critical into develop efficient methods for modeling practical processes, where such complexities are commonly encountered, and to validate the models and improve the accuracy of the predicted results.

A wide range of numerical methods is available for solving the governing equations. For 2D and axisymmetric problems, the pressure may be eliminated to obtain the

vorticity equation (Jaluria and Torrance, 2003). The stream function, vorticity and energy equations can then be solved using a non-uniform grid, with finer grids located in regions where large gradients are expected. Figure 5 shows a typical mesh for the fiber drawing process. The perform typically goes from a diameter of around 10 cm to the fiber diameter of 125 $\mu$m in a distance of around 0.3 m. Thus, extra care has to be exercised near the bottom of the region to avoid highly distorted grids due to the small diameter of the fiber. The optimal grid can be obtained by numerical experimentation. For instance, a 369 $\times$ 41 (axial and radial, respectively) grid for the fiber/preform and a 369 $\times$ 61 grid for the purge gases in fiber drawing with a single layer was found to be adequate. Successive under-relaxation is generally needed to obtain convergence for the strongly non-linear problem with strong temperature-dependent properties. For 3D problems, the primitive variables $\overline{V}$ and $T$ are used more efficiently (Minkowycz and Sparrow, 1997; Patankar, 1980).

The strong variation of viscosity with temperature makes it necessary to employ very fine grids, linearization and decoupling of the equations, and iterative procedures, using a variety of numerical techniques. Even a change of a few degrees in temperature in the vicinity of the softening point of glass can cause substantial change in viscosity and thus in the flow field and the neck-down profile. Similar considerations apply for polymer extrusion and other thermal processes where strong property changes may occur. Large drawing speeds in fiber drawing, screw rotational speed in screw extrusion, or wire speed in coating place very stringent demands on the numerical scheme and on the imposition of appropriate boundary conditions. Figure 6 shows the general configuration of the system for the coating of a wire or a fiber. The wire moves at relatively-high speed at the center and the fluid, which is often a polymer, is dragged along with the wire, ultimately resulting in a fine coating around the wire. The polymer is contained in a chamber, often called the applicator, which may be pressurized, and an exit die is used to control the coating

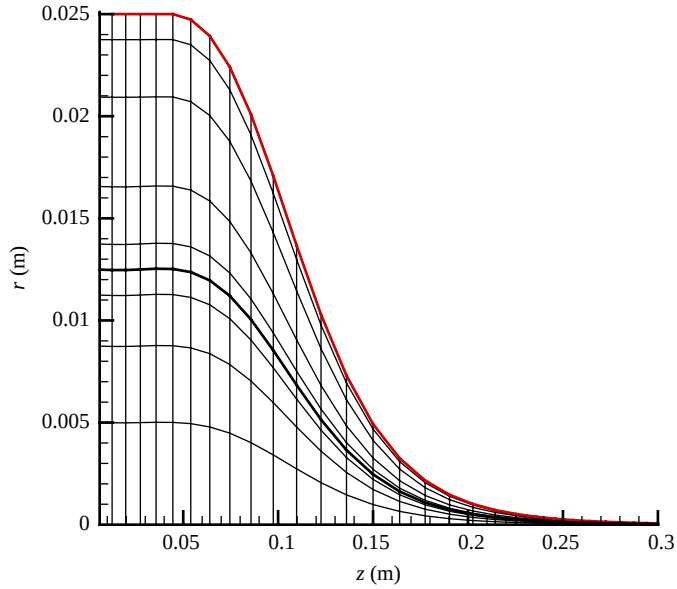


**Figure 5.**
Typical grid in a fiber drawing process

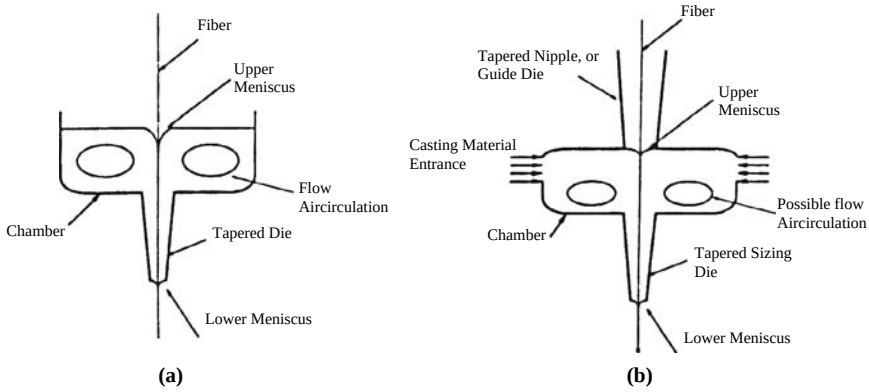


**Figure 6.**
(a) Open-cup and (b) pressurized cup coating process for wires and fibers

diameter and uniformity. Thus, three regions, consisting of a region very close to the wire or fiber, the bulk fluid and the die can be defined and appropriate grids developed for these. Figure 7 shows a typical grid system that couples the three regions and that can be used to accurately model the process.

## 3. Results

The preceding aspects of material property variation, complex domains, complicated boundary conditions and unknown boundaries are encountered in a wide range of practical problems (Jaluria, 2001, 2003). Only a few typical results are presented here to illustrate the corresponding numerical simulation.

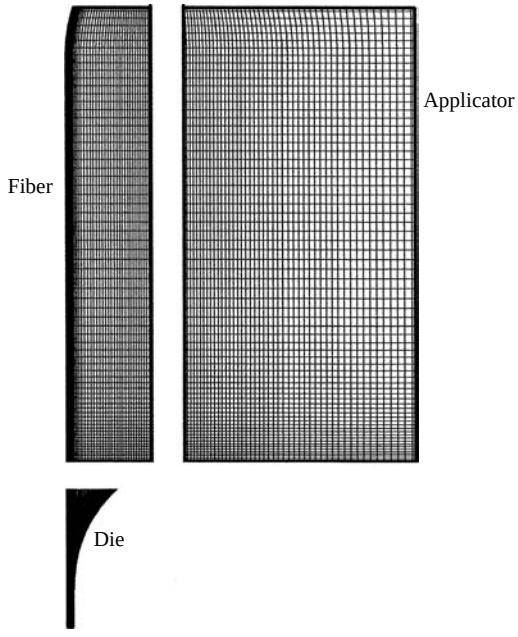


**Figure 7.**
Grids in the three regions that make up a coating applicator and die system

*3.1 Optical fiber drawing*

The optical fiber drawing process outlined earlier involves many of these concerns. Figure 8 shows typical computed results on the temperature field in the neck-down region for three furnace lengths. The glass flow is smooth and well layered because of the high viscosity. A typical temperature difference of order 100°C arises across the fiber for preform diameters of around 5 cm. However, even this small difference is an important factor in fiber quality and characteristics because of the large, exponential, dependence of viscosity on the temperature. It affects the neck-down shape and the generation of temperature-induced defects. Larger temperature differences arise for larger preform diameters. Viscous dissipation, though relatively small, is mainly concentrated near the end of the neck-down and must be incorporated in the model since it plays an important role in maintaining the temperatures above the softening point.

The fiber drawing process involves modeling the free surface flow of glass under large temperature differences and large changes in viscosity and cross-sectional area. A solution of the transport equations, along with a surface force balance, is needed for

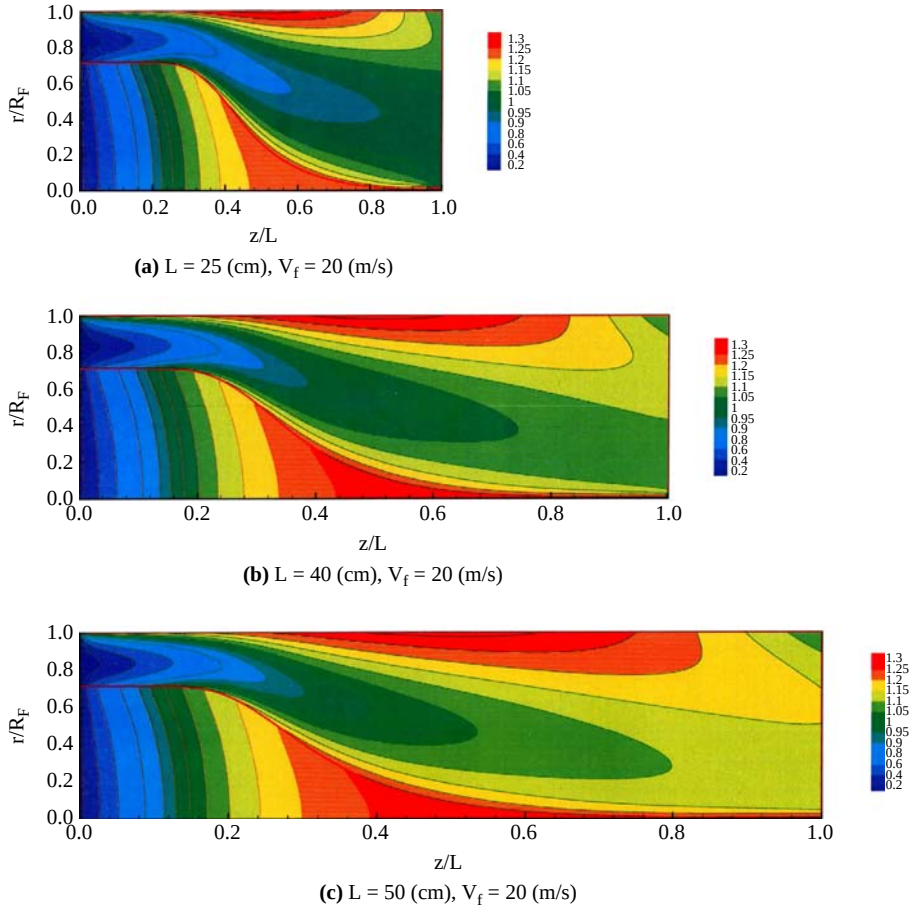


**(a)** L = 25 (cm), $V_f$ = 20 (m/s)

**(b)** L = 40 (cm), $V_f$ = 20 (m/s)

**(c)** L = 50 (cm), $V_f$ = 20 (m/s)

**Figure 8.**
Calculated temperature field in the glass during drawing of single-layer optical fiber for three furnace lengths

the determination of the neck-down profile, as mentioned earlier. The normal force balance and the vertical momentum equations are used to obtain a correction scheme for the neck-down profile. After a new corrected profile is obtained, the governing equations are solved for the flow and heat transfer, considering both radiation and convection transport, and the force balance is again invoked. This iterative process is continued until the neck-down shape does not change from one iteration to the next. It is found that viscous and gravitational forces are dominant in the determination of the profile. Surface tension effects are small, even though they are important in many other free boundary flows.

A typical example of the numerically calculated neck-down profile for a two-layer optical fiber is shown in Figure 9. Initially, the optically thick assumption is used to obtain the profile. Then the zonal method is used to more accurately calculate the radiative heat transfer and the profile is corrected. In most cases, the neck-down profile is quite unrealistic during the first few iterations. But after a few iterations, the shape becomes smooth and monotonically decreasing, eventually reaching a steady, converged, profile, indicated by the invariance of the profile with further iterations. For convergent cases, perturbations to the initial profile and different starting shapes lead to the converged neck-down profile, indicating the robustness of the scheme and the stability of the drawing process (Roy Choudhury *et al.*, 1999). The force balance conditions are also closely satisfied if the iterations converge. For the double-layer perform/fiber, the force balance conditions are checked at all the interfaces and the radiation calculations are much more involved. For further details on this model, see Chen and Jaluria (2004).

### *3.2 Fiber coating*

As shown in Figure 6, the coating of a wire or fiber with a jacketing material for protection against abrasion and for increased strength is another important process. The temperatures in the process are limited by the properties of the coating material used.

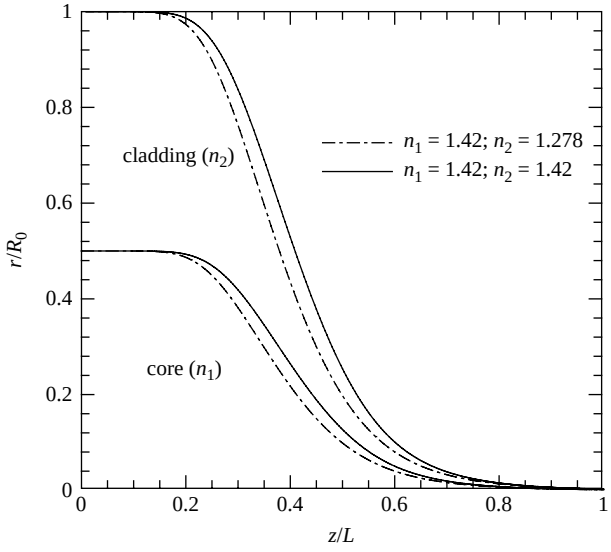


**Figure 9.**
Calculated neck-down profiles for a perform with a core-cladding structure at two values of the refractive index of the outer layer

For commercial curable acrylates, this temperature generally cannot exceed 150°C. The wet coating may then cured by ultra-violet radiation. In addition, the fluid is generally non-Newtonian and the properties, particularly viscosity, vary strongly with temperature. The geometry is complicated, as discussed earlier in terms of the discretization, and a free surface flow arises at the exit, giving rise to a meniscus, as shown in Figure 6. Viscous shear due to the moving wire or fiber results in a circulatory fluid motion within the fluid. A balance between surface tension, viscous, gravitational, and pressure forces results in an upstream meniscus at the cup entrance. A downstream meniscus at the die exit results primarily from a balance between viscous and inertia forces, the surface tension being a relatively small effect. Interest lies in obtaining concentric coatings, of uniform thickness, and free of particle inclusions or bubbles (Paek, 1986).

The use of high-draw rates requires consideration of alternate pressurized applicator designs, where pressure induced motion of the coating material is used to reduce the shear at the fiber surface and establish a stable free surface flow (Simpkins and Kuck, 2000; Ravinutala *et al.*, 2000). It was found that, the upstream meniscus does not significantly affect the overall flow in the applicator, though the flow close to the meniscus is strongly affected by the shape of the meniscus. An additional benefit resulting with such pressurized dies has been the minimizing of gas bubbles entrained at the coating cup entrance and then trapped within the coating layer. The numerical simulation considered different designs and geometries of the applicator as well as of the die (Rattan and Jaluria, 2003; Yoo and Jaluria, 2004). Of particular interest was the effect of the meniscus on the overall flow, the flow field in the vicinity of the entrance and the exit, the mass flow rate of the fluid at the exit leaving with the fiber and the effect of pressurization. Different fiber speeds were considered and the coating material considered was glycerin, as employed in experiments. Figure 10 show typical results

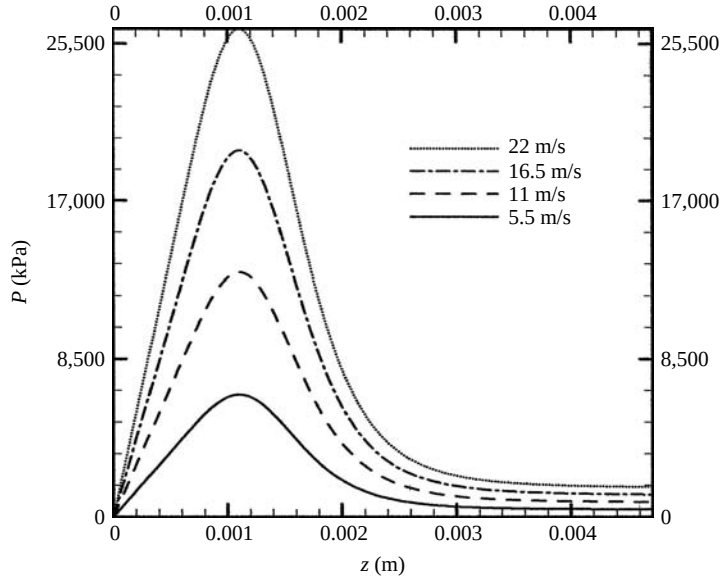


**Figure 10.**
Pressure distribution in the exit die for polymer coating of a moving wire or fiber under isothermal conditions

obtained in terms of the pressure distribution in the exit die for isothermal conditions. It is seen that a maximum arises somewhere near the mid section of the die. This pressure was found to be much larger that the pressure typically imposed at the fluid inlet to the applicator. Thus, the exit conditions are largely dominated by the die shape and wire speed, rather than the pressure in the applicator chamber. A properly designed die can help in controlling the thickness and quality of the coating. Thermal effects can also have a strong effect on the flow due to the dependence of fluid properties on temperature. The corresponding pressure distribution when thermal effects, due to heat transfer from the fiber, viscous dissipation and heat loss to the surroundings are included, is shown in Figure 11. The pressures were found to decrease as the temperatures increase due to the reduction in fluid viscosity. The flow was also found to be more stable, leading to greater uniformity of the coating, as the temperatures were increased. Thus, the thermal conditions at the boundaries can be used to affect the coating characteristics.

Another important aspect in this process is the exit meniscus, which represents the profile of the free surface as the fluid exits from the die due to the viscous drag from the moving wire or fiber (Blyler and DiMarcello, 1980). An approach similar to that mentioned earlier in connection with the optical fiber drawing process may be used. Thus, the governing equations are solved to obtain the temperature and flow distributions, from which the shear at the free surface is determined. The additional forces due to gravity, surface tension and outside shear due to air are included to determine the overall force balance. The imbalance is used to iterate, starting with a guessed profile, till the force balance is satisfied and a converged meniscus is obtained (Yoo and Jaluria, 2008). Figure 12 shows the results obtained numerically and compares these with experimental data on the profile (Raj, 2004). A fairly good agreement is observed, indicating the validity and accuracy of this approach.

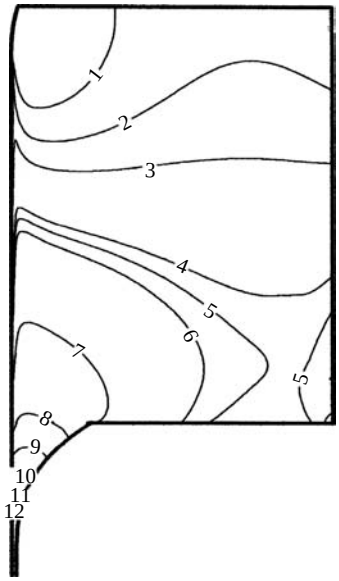


| Level | *P* |
|---|---|
| 12 | 119.605 |
| 11 | 71.7239 |
| 10 | 30.2121 |
| 9 | 18.3854 |
| 8 | 11.8902 |
| 7 | 7.67639 |
| 6 | 6.67665 |
| 5 | 6.58405 |
| 4 | 6.51028 |
| 3 | 6.12641 |
| 2 | 5.88472 |
| 1 | 5.44346 |

**Figure 11.**
Calculated pressure distribution in the applicator/die system for the coating process when thermal effects are included

*3.3 Cooling of electronic systems*

As another example of a practical problem where property variations and boundary conditions are important, consider the flow in a channel with isolated, protruding, heat sources, as shown in Figure 13. This configuration represents an electronic system, with the heat sources representing electronic components, such as chip assemblies consisting of the chip and a thermal sink. Conjugate conditions exist at the boundary between the cooling fluid and the solid substrate. Boundary conditions have also to be imposed at the openings through which the fluid enters or leaves the system. The geometry can be complicated due to the positioning and dimensions of the sources and the cooling flow configuration. The governing equations are similar to those given earlier and buoyancy effects and radiation may be important in some cases.

Figure 14 shows a comparison between the computed temperature distributions for a 2D natural convection flow due to two sources located in a channel, as shown in Figure 13. An experimental study using the Filtered Rayleigh Scattering (FRS) technique is employed to obtain the temperature profiles above the thermal sources (Bogusko *et al.*, 2002). However, the experimental study employed a channel open on all sides and the walls were unheated. The separation between the walls was much less than the width and length of the channel. The challenge was to simulate this experiment to obtain similar trends in the predictions. The numerical results are compared with the FRS measurements in Figure 14 for the region above the two sources, indicating good agreement. Here, $\theta$ is the nondimensional temperature $(T - T_a)/(T_s - T_a)$, where s represents the source and a the ambient temperature. It is found that adiabatic, or perfectly insulated, conditions at the walls of the channel approximate the experiment much better than isothermal conditions. Developed flow

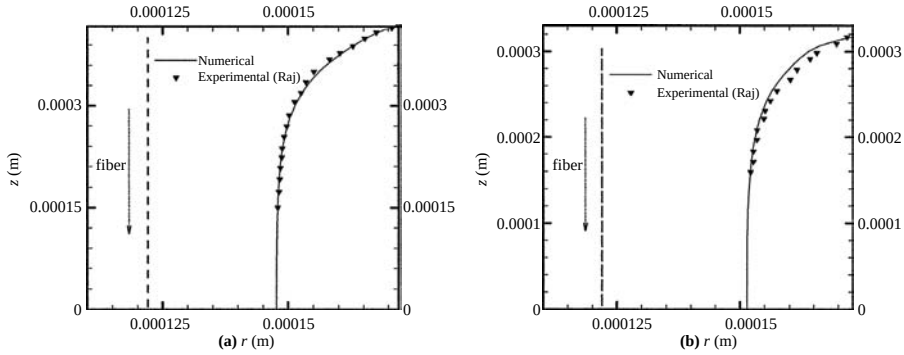


**Figure 12.**
Calculated exit meniscus in the coating process, along with experimental measurements of the profile, for glycerine at fiber speeds of: (a) 20 and (b) 75 m/min

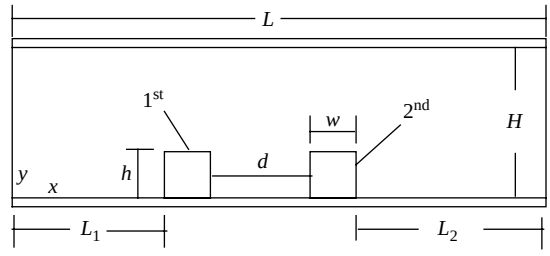


**Figure 13.**
Isolated protruding heat sources in a channel with openings

conditions were assumed at the openings and this seemed to be a satisfactory approximation (Icoz and Jaluria, 2005). Clearly, the numerical simulation of the boundary conditions is an important consideration and comparisons with existing data could be used effectively to obtain the most accurate model.

The importance of including property variations is demonstrated in the results shown in Figure 15(a). These results pertain to the flow in a channel with a portion of the bottom heated, the remaining being adiabatic (Wang *et al.*, 2003; Wang and Jaluria, 2004). A 3D simulation is carried out. The geometry is fairly simple and the boundary conditions are also not complicated. But a 3D simulation is needed to determine transverse variations due to instabilities that may arise. Figure 15(a) shows the results obtained by considering the fluid properties as constant at four reference temperatures and also by treating the variable property (VP) case. The reference temperatures are taken as inlet temperature $T_o$, integrated temperature $T_{int}$, the film temperature $T_f$, and the temperature of the heat source $T_H$. Even though the film temperature and the integrated value come close to the VP results, it is evident that considerable error may result if an arbitrary reference temperature is taken and that the simulation of the VP

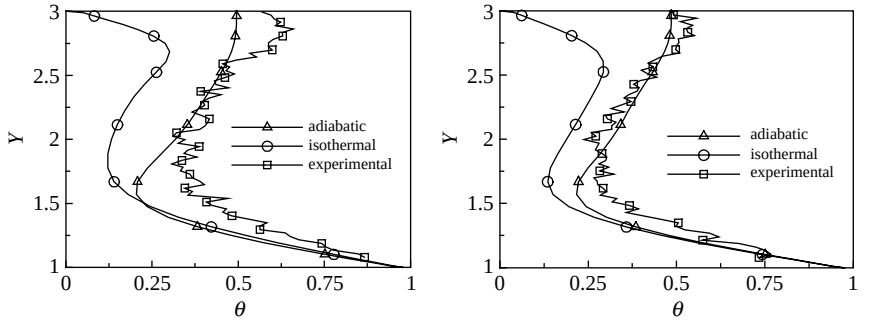


**Figure 14.**
Comparisons between numerical predictions and experiments for temperature distributions above the two sources in natural convection from two isolated sources in a channel open on all sides

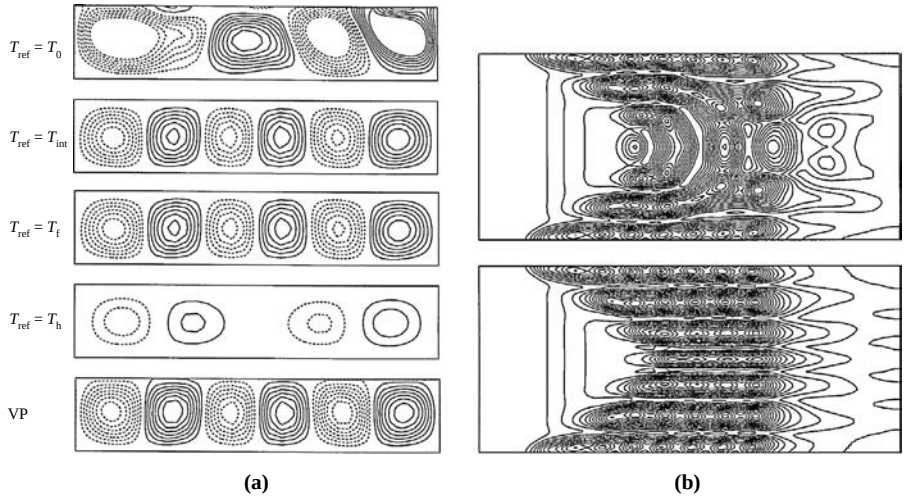


**Figure 15.**
Longitudinal vortices in channel flow with a portion of the bottom surface heated: (a) results as seen from the side for constant properties at different reference temperatures and from the variable property solution; (b) flow field from the top showing the 3D nature of the flow

case is the appropriate approach. The corresponding 3D results are quite involved, as shown in Figure 15(b), indicating the existence of longitudinal vortices and inability of a 2D model to accurately capture the transport process.

*3.4 Validation*

A crucial consideration in modeling and simulation of practical processes is that of validation because of the simplifications used to treat various complexities mentioned earlier. It is important to ensure that the numerical code performs satisfactorily and that the model is an accurate representation of the physical problem. These aspects are sometimes referred to as verification and validation, respectively, (Roache, 1998). Unless the models are satisfactorily validated and the accuracy of the predictions established, the models cannot be used as a basis for design and optimization (Jaluria, 1998). Validation is often based on a consideration of the physical behavior of the results obtained and comparisons with available analytical and numerical results. Comparisons with experimental results are desirable, though lack of experimental data may, in some cases, require the development of an experimental arrangement for providing inputs for validation. Figure 16 shows the comparisons between numerical results from several studies (Yoo and Jaluria, 2002; Chiu and Jaluria, 2000; Mahajan and Wei, 1991) and an experimental study (Eversteyn *et al.*, 1970). It is interesting to note that, despite substantial differences in the models and in the property evaluations, the numerical and experimental results show fairly good agreement. This is quite typical in a variety of practical processes, where the overall features are not very sensitive to the model. However, the velocity, temperature and pressure distributions may be quite sensitive and should then be used to select the most accurate model.

Similarly, experiments have been carried to validate models for twin-screw extrusion, particularly the transport in the intermeshing region, as shown in Figure 17. An experimental system consisting of rotating cylinders was developed and the characteristics of the flow and the basic features of the mixing process in the

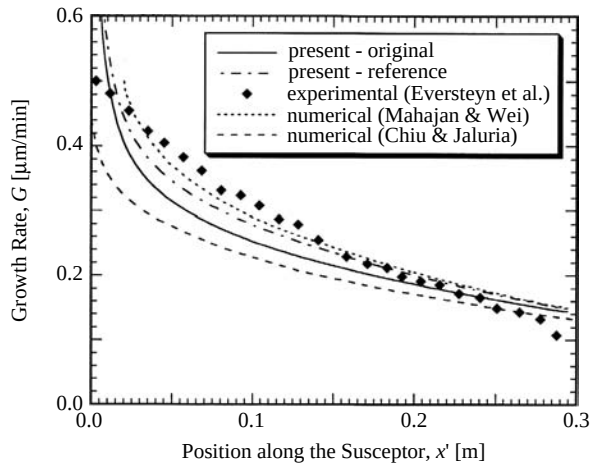


**Figure 16.**
Comparison between numerical predictions and experiments for chemical vapor deposition of silicon in a horizontal reactor

intermeshing, or mixing, region were investigated (Sastrohartono *et al.*, 1990). Experimentally and numerically obtained streamlines in the region between two rotating cylinders, approximating a twin-screw, are shown, indicating good agreement. Some of the fluid flowing adjacent to the left cylinder continues to flow along its surface, while the remaining flows over to the other cylinder. A flow division ratio $x_f$, defined as the fraction of the mass flow that crosses over from one channel to the other, is taken as a measure of mixing and is determined by using the dividing streamline that separates the two fluid streams. A comparison between experimental and numerical results is shown, indicating good agreement at the typically small Reynolds numbers encountered in extruders. A small difference, between numerical and experimental results, arises as Reynolds numbers increase beyond 1.0, because of significant inertia effects, which are neglected in the mathematical model. For more detailed comparisons, velocity and temperature distributions have been obtained using more elaborate experimental systems in this process and in others and compared with the numerical results (Jaluria, 2003).

## 4. Conclusions

This paper presents the important considerations in the numerical simulation of practical processes that involve complicated domains, large property changes, combined mechanisms and intricate boundary conditions. The transformation of the domain into a simpler one by means of coordinate transformations or approximations is discussed. Concerns with discretization in these cases are also discussed. The complexity introduced due to strong property variations and the stringent demands placed on the numerical scheme, particularly in terms of the nonlinearity and coupling of the governing equations, are discussed. Moving boundaries, free surfaces and conjugate boundary conditions require particular care for accurate simulations. Some of the basic approaches that may be adopted for these transport processes are presented. Validation of the model in terms of existing results, as well as new experimental data, is outlined. Results for a few important practical problems are presented to illustrate the use of these approaches, as well as some of the major concerns that arise.

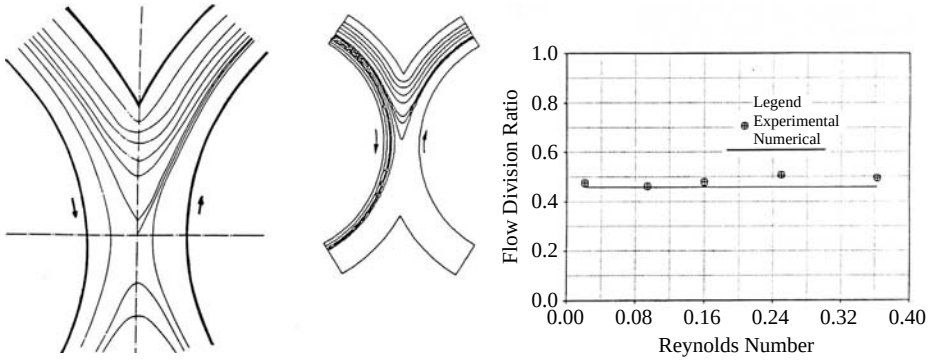


**Figure 17.**
Comparisons between numerical modeling and experimental results for the mixing region of a twin-screw polymer extruder

## References

Blyler, L.L. and DiMarcello, F.V. (1980), "Fiber drawing, coating and jacketing", *Proc. IEEE*, Vol. 68, pp. 1194-8.

Bogusko, M., Elliot, G. and Carter, C. (2002), "Filtered Rayleigh scattering for fluid/thermal system", paper presented at 22nd AIAA Aerodyn. Measurement Tech. Ground Testing Conf., St Louis, Missouri, p. 3233.

Chen, C. and Jaluria, Y. (2004), "Numerical simulation of transport in optical fiber drawing with core-cladding structure", *Proc. ASME Heat Transfer/Fluids Engg. Summer Conf., Charlotte, NC*.

Chiu, W.K.S. and Jaluria, Y. (2000), "Continuous chemical vapor deposition processing with a moving finite thickness susceptor", *J. Mater. Res.*, Vol. 15, pp. 317-28.

Eversteyn, F.C., Severin, P.J.W., Brekel, C.H.J. and Peek, H.L. (1970), "A stagnant layer model for the epitaxial growth of silicon from silane in a horizontal reactor", *J. Electrochem. Soc.*, Vol. 117, pp. 925-31.

Icoz, T. and Jaluria, Y. (2005), "Numerical simulation of boundary conditions and the onset of instability in natural convection due to protruding thermal sources in an open rectangular channel", *Numerical Heat Transfer*, Vol. 48, pp. 831-47.

Jaluria, Y. (1992), "Transport from continuously moving materials undergoing thermal processing", *Ann. Rev. Heat Transfer*, Vol. 4, pp. 187-245.

Jaluria, Y. (1996), "Heat and mass transfer in the extrusion of non-Newtonian materials", *Advances in Heat Transfer*, Vol. 28, pp. 145-230.

Jaluria, Y. (1998), *Design and Optimization of Thermal Systems*, McGraw-Hill, New York, NY.

Jaluria, Y. (2001), "Fluid flow phenomena in materials processing – the 2000 freeman scholar lecture", *ASME J. Fluids Engg.*, Vol. 123, pp. 173-210.

Jaluria, Y. (2003), "Thermal processing of materials: from basic research to engineering", *J. Heat Transfer*, Vol. 125, pp. 957-79.

Jaluria, Y. and Torrance, K.E. (2003), *Computational Heat Transfer*, 2nd ed., Taylor & Francis, New York, NY.

Jensen, K.F., Einset, E.O. and Fotiadis, D.I. (1991), "Flow phenomena in chemical vapor deposition of thin films", *Ann. Rev. Fluid Mechanics*, Vol. 23, pp. 197-232.

Lee, S.H.K. and Jaluria, Y. (1996), "Simulation of the transport processes in the neck-down region of a furnace drawn optical fiber", *Int. J. Heat Mass Transfer*, Vol. 40, pp. 843-56.

Li, T. (Ed.) (1985), *Optical Fiber Communications, Vol. 1: Fiber Fabrication*, Academic Press, New York, NY.

Lin, P. and Jaluria, Y. (1998), "Conjugate thermal transport in the channel of an extruder for non-Newtonian fluids", *Int. J. Heat Mass Transfer*, Vol. 41, pp. 3239-53.

Mahajan, R.L. (1996), "Transport phenomena in chemical vapor-deposition systems", *Advances in Heat Transfer*, Vol. 28, pp. 339-425.

Mahajan, R.L. and Wei, C. (1991), "Buoyancy, Soret, Dufour and variable property effects in silicon epitaxy", *J. Heat Transfer*, Vol. 113, pp. 688-95.

Minkowycz, W.J. and Sparrow, E.M. (Eds) (1997), *Advances in Numerical Heat Transfer*, Vol. 1, Taylor & Francis, Washington, DC.

Paek, U.C. (1986), "High speed high strength fiber coating", *J. Lightwave Tech.*, Vol. LT-4, pp. 1048-59.

Paek, U.C. (1999), "Free drawing and polymer coating of silica glass optical fibers", *J. Heat Transfer*, Vol. 121, pp. 775-88.

Patankar, S.V. (1980), *Numerical Heat Transfer and Fluid Flow*, Taylor & Francis, Philadelphia, PA.

Raj, A. (2004), "Pressure effects on the exit meniscus of an optical fiber coating applicator", MS thesis, Rutgers University, New Brunswick, NJ.

Rattan, K. and Jaluria, Y. (2003), "Simulation of the flow in a coating applicator for optical fiber manufacture", *Computational Mechanics*, Vol. 31, pp. 428-36.

Ravinutala, S., Rattan, K., Polymeropoulos, C.E. and Jaluria, Y. (2000), "Dynamic menisci in a pressurized fiber applicator", *Proc. 49th Int. Wire Cable Symp., Atlantic City, NJ*.

Roache, P.J. (1998), *Verification and Validation in Computational Science and Engineering*, Hermosa Publishers, Albuquerque, NM.

Roy Choudhury, S., Jaluria, Y. and Lee, S.H.K. (1999), "Generation of neck-down profile for furnace drawing of optical fiber", *Numerical Heat Transfer*, Vol. 35, pp. 1-24.

Sastrohartono, T., Esseghir, M., Kwon, T.H. and Sernas, V. (1990), "Numerical and experimental studies of the flow in the nip region of a partially intermeshing co-rotating twin screw extruder", *Polymer Engg. Sci.*, Vol. 30, pp. 1382-98.

Simpkins, P. and Kuck, V. (2000), "Air entrapment in coatings via tip streaming meniscus", *Nature*, Vol. 403, pp. 641-3.

Tadmor, Z. and Gogos, C. (1979), *Principles of Polymer Processing*, Wiley, New York, NY.

Wang, Q. and Jaluria, Y. (2004), "Three dimensional conjugate heat transfer in a horizontal duct with discrete heating", *J. Heat Transfer*, Vol. 126, pp. 642-7.

Wang, Q., Yoo, H. and Jaluria, Y. (2003), "Convection in a horizontal duct under constant and variable property formulations", *Int. J. Heat Mass Transfer*, Vol. 46, pp. 297-310.

Yin, Z. and Jaluria, Y. (1997), "Zonal method to model radiative transport in an optical fiber drawing furnace", *J. Heat Transfer*, Vol. 119, pp. 597-603.

Yoo, H. and Jaluria, Y. (2002), "Thermal aspects in the continuous chemical vapor deposition of silicon", *J. Heat Transfer*, Vol. 124, pp. 938-46.

Yoo, S.Y. and Jaluria, Y. (2004), "Numerical study of flow in an optical fiber coating process", *Proc. 53rd Int. Wire Cable Symp., Philadelphia, PA*, pp. 371-5.

Yoo, S.Y. and Jaluria, Y. (2008), "Numerical simulation of the meniscus in non-isothermal free surface flow at the exit of a coating die", *Numerical Heat Transfer*, Vol. 53 No. 2, pp. 111-31.

**Corresponding author**
Yogesh Jaluria can be contacted at: jaluria@jove.rutgers.edu